Journal Pre-proof

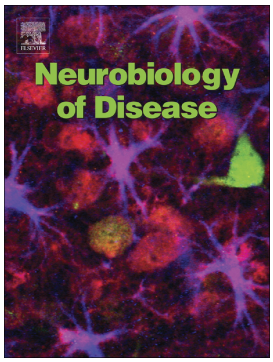

Knockdown of GADD34 in neonatal mutant SOD1 mice ameliorates ALS

Ghanashyam D. Ghadge, Yoshifumi Sonobe, Adrian Camarena, Claire Drigotas, Frank Rigo, Karen K. Ling, Raymond P. Roos

PII: S0969-9961(19)30377-8

DOI: https://doi.org/10.1016/j.nbd.2019.104702

Reference: YNBDI 104702

To appear in: *Neurobiology of Disease*

Received date: 24 September 2019

Revised date: 26 November 2019

Accepted date: 8 December 2019

Please cite this article as: G.D. Ghadge, Y. Sonobe, A. Camarena, et al., Knockdown of GADD34 in neonatal mutant SOD1 mice ameliorates ALS, *Neurobiology of Disease*(2019), https://doi.org/10.1016/j.nbd.2019.104702

This is a PDF file of an article that has undergone enhancements after acceptance, such as the addition of a cover page and metadata, and formatting for readability, but it is not yet the definitive version of record. This version will undergo additional copyediting, typesetting and review before it is published in its final form, but we are providing this version to give early visibility of the article. Please note that, during the production process, errors may be discovered which could affect the content, and all legal disclaimers that apply to the journal pertain.

© 2019 Published by Elsevier.

Journal Pre-proof

Knockdown of GADD34 in neonatal mutant SOD1 mice ameliorates ALS

Ghanashyam D. Ghadge[a,1], Yoshifumi Sonobe[a,1], Adrian Camarena[a], Claire Drigotas[a], Frank Rigo[b], Karen K. Ling[b], Raymond P. Roos[a,*]

[a]Department of Neurology, University of Chicago Medical Center, Chicago, IL 60637
[b]Ionis Pharmaceuticals, Carlsbad, CA 90201

Journal Pre-proof

[1]These authors contributed equally.
*Corresponding author at: Department of Neurology, University of Chicago Medical Center, 5841 S. Maryland Ave./MC2030, Chicago, IL 60637
Email address: rroos@neurology.bsd.uchicago.edu (R.P. Roos)

Abstract

Mutations in Cu/Zn superoxide dismutase (SOD1) cause ~20% of familial ALS (FALS), which comprises 10% of total ALS cases. In mutant SOD1- (mtSOD1-) induced ALS, misfolded aggregates of SOD1 lead to activation of the unfolded protein response/integrated stress response (UPR/ISR). Protein kinase R (PKR)-like endoplasmic reticulum kinase (PERK), a kinase that phosphorylates eukaryotic translation initiator factor 2α (p-eIF2α), coordinates the response by causing a global suppression of protein synthesis. Growth arrest and DNA damage 34 (GADD34) dephosphorylates p-eIF2α, allowing protein synthesis to return to normal. If the UPR/ISR is overwhelmed by the amount of misfolded protein, CCAAT/enhancer-binding homologous protein (CHOP) is activated leading to apoptosis. In the current study we investigated the effect of knocking down CHOP and GADD34 on disease of G93A and G85R mtSOD1 mice. Although a CHOP antisense oligonucleotide had no effect on survival, an intravenous injection of GADD34 shRNA encoded in adeno-associated virus 9 (AAV9) into neonatal G93A as well as neonatal G85R mtSOD1 mice led to a significantly increased survival. G85R mtSOD1 mice had a reduction in SOD1 aggregates/load, astrocytosis, and microgliosis. In contrast, there was no change in disease phenotype when GADD34 shRNA was delivered to older G93A mtSOD1 mice. Our current study shows that GADD34 shRNA is effective in ameliorating disease when administered to neonatal mtSOD1 mice. Targeting the UPR/ISR may be beneficial in mtSOD1-induced ALS as well as other neurodegenerative diseases in which misfolded proteins and ER stress have been implicated.

Journal Pre-proof

Keywords: Familial amyotrophic lateral sclerosis; mutant Cu/Zn superoxide dismutase; unfolded protein response; integrated stress response; CHOP; GADD34; antisense oligonucleotides; shRNA

Journal Pre-proof

Introduction

Amyotrophic lateral sclerosis (ALS) is a progressive neurodegenerative disease characterized by the selective loss of motor neurons, with death ensuing 3-5 years after the onset. Approximately 10% of ALS cases are familial (FALS), usually exhibiting a dominant inheritance pattern, with ~20% of FALS cases caused by mutant Cu/Zn superoxide dismutase (mtSOD1). Although mtSOD1 is only responsible for a fraction of ALS cases, transgenic mtSOD1 mice have served as a useful model to study the pathogenesis of the disease. Evidence suggests that mtSOD1 causes FALS through a toxic gain of function rather than a loss of function, likely due to misfolded protein aggregates that accumulate in the cytoplasm (Kikuchi et al., 2006; Taylor et al., 2016).

Misfolded aggregated protein, which is a feature of both sporadic ALS, FALS, and other neurodegenerative diseases, has generated interest in targeting the unfolded protein response /integrated stress response (UPR/ISR) as a potential treatment of ALS (Walker and Atkin, 2011). The UPR involves three stress sensors in the endoplasmic reticulum (ER): protein kinase R (PKR)-like endoplasmic reticulum kinase (PERK), activating transcription factor 6 (ATF6), and inositol-requiring kinase-1 (IRE1). As misfolded proteins accumulate in the cytoplasm, these sensors induce the UPR. PERK is the most rapidly activated of the three sensors, and phosphorylates eukaryotic translation initiator factor 2 on the α-subunit (eIF2α) (Ron and Walter, 2007). Phosphorylated eIF2α (p-eIF2α), which coordinates the ISR, inhibits most cellular translation, while selectively promoting the translation of cytoprotective genes that enhance protein folding or aid in the degradation of misfolded proteins (Hinnebusch et al., 2016). When eIF2α is phosphorylated, activating transcription factor 4 (ATF4) is upregulated, which promotes the transcription of genes involved in chaperone function and protein degradation. ATF4 in turn upregulates growth arrest and DNA damage 34 (GADD34) protein and CCAAT/enhancer-binding homologous protein (CHOP). GADD34 is a phosphatase that dephosphorylates p-eIF2α, effectively ending the UPR and allowing the cell to resume normal protein synthesis (Reid et al., 2016). If the UPR is overwhelmed by misfolded proteins and is unable to adequately protect the cell during times of stress, CHOP induces cellular apoptosis and autophagy (Ron and Walter, 2007).

Our previous genetic studies in G85R-SOD1 mice suggested that the UPR/ISR plays a role in mitigating damage caused by mtSOD1. Transgenic mtSOD1 mice crossed with PERK haploinsufficient mice have decreased phosphorylation of eIF2α, accelerated disease onset, accelerated pathology, increased SOD1 aggregation, and shorter survival than mtSOD1 mice with normal levels of PERK (Wang et al., 2011). Furthermore, transgenic mtSOD1 mice with reduced GADD34 function have enhanced phosphorylation of eIF2α, prolongation in disease onset, decreased disease pathology, and longer survival than mtSOD1 mice with normal levels of GADD34 (Wang et al., 2014a). These results implicated the UPR/ISR as a target for therapy in ALS, prompting the present studies testing the effect of an antisense oligonucleotide (ASO) that knocks down CHOP and a shRNA that knocks down GADD34 in mtSOD1 transgenic mice. CHOP knockdown showed no effect on disease in G93A and G85R mtSOD1-induced ALS.

GADD34 shRNA ameliorated disease in neonatal G93A-SOD1 and G85R-SOD1 transgenic mice, but not adult G93A-SOD1 mice.

Journal Pre-proof

Materials and Methods

Mice

Animal experiments were performed in compliance with the NIH Guide for the Care and Use of Laboratory Animals, and with the approval of the University of Chicago Institutional Animal Care and Use Committee. G93A-SOD1 and G85R-SOD1 transgenic mice on a C57BL/6J background (Bruijn et al., 1997; Wooley et al., 2005) were obtained from Jackson Labs (Bar Harbor, ME). Mice were genotyped for human SOD1 by PCR using the following primers (forward, 5'-CATCAGCCCTAATCCATCTGA-3'; reverse, 5'-CGCGACTAACAATCAAAGTGA-3'). An approximately equal number of male and female mice were used for the study since no difference in their clinical phenotype was observed in a previous study (Ghadge et al., 2019; Wooley et al., 2005), as well as the present one.

CHOP ASO

Sequences of the control ASO and CHOP ASOs are listed in Table 1. All chemically modified oligonucleotides were synthesized and purified as previously described (Swayze et al., 2007). The ASOs were 20 nucleotides in length, wherein the central gap segment comprising ten 2'-deoxyribonucleotides that are flanked on the 5' and 3' wings by five 2'MOE modified nucleotides. Internucleotide linkages were phosphorothioate interspersed with phosphodiester, and all cytosine residues were 5'-methylcytosines. The CHOP ASOs that were most potent in target knockdown in cell culture were further confirmed in mice. To identify the most effective CHOP ASOs in the context of ER stress, we tested the effect of the ASOs on ER stress produced by a tunicamycin injection in the lateral ventricle (Chen et al., 2012). In these experiments, 400 μg of the ASO was injected intracerebroventricular (i.c.v.) into 7-8 weeks old wild type C57BL/6J mice. Two weeks later, 5 μg tunicamycin was injected i.c.v. to induce ER stress. The mice were euthanized 3 days later and the knockdown of CHOP was assessed.

To test the effect of CHOP knockdown on survival in mtSOD1 mouse models of ALS, 400 μg of the CHOP ASO was injected i.c.v. into G93A-SOD1 mice when 75 and 105 days of age, and into G85R-SOD1 mice, when 250 days of age. The ASOs were prepared and injected as describe (Ling et al., 2018, Rigo et al., 2014).

GADD34 shRNA

We tested two shRNAs that had previously been shown by the Broad Institute to knock down GADD34 by 55% (now termed GADD34-shRNA-55) and 95% (now termed GADD34-shRNA) (MilliporeSigma, St. Louis, MO). These shRNAs were cloned into an AAV shuttle vector pFB-U6-shRNA-polyT-CMV-GFP-polyA (pFB) (Virovek Inc., Hayward, CA). Cells expressing the control or GADD34 shRNA also expressed GFP from a different promoter.

To test the effect of the shRNAs on GADD34 knockdown, NSC-34 cells, which are a motor neuron-like cell line, were transfected using Lipofectamine LTX (Invitrogen, Carlsbad, CA) with 0.5 μg of pFB plasmids expressing Control-shRNA or a GADD34 shRNA. The cells were cultured for 48h, and then treated with 500 nM thapsigargin (MilliporeSigma) for either 24 hours or as indicated to trigger ER stress. The cells were then processed with TRIzol (Invitrogen), and the RNA obtained was processed for RT-PCR. For Western blot analysis, NSC-34 cells were lysed at 24 hours or indicated time points following thapsigargin treatment

with a lysis buffer consisting of 4 M urea, 0.5% SDS, cOmplete Mini EDTA-free protease inhibitors (MilliporeSigma), and a phosphatase inhibitor cocktail (MilliporeSigma).

Self-complementary adeno-associated virus 9 (AAV) vectors were prepared by Virovek Inc. that encoded the shRNAs: AAV:Control-shRNA, AAV:GADD34-shRNA-55, and AAV:GADD34-shRNA. To test the effect of GADD34 shRNA, neonatal C57BL/6J mice were injected intravenously with $5X10^{11}$ genome copies of the recombinant AAVs. Eighty one days later, these mice were i.c.v. injected with 5 μg of tunicamycin to trigger ER stress. The mice were euthanized 3 days later to collect the spinal cord and assess the knockdown.

In order to test the effect of GADD34-shRNA on disease, neonatal (P1) G93A and G85R mtSOD1 mice or ~120-days-old G93A-SOD1 mice were injected intravenously with $5X10^{11}$ genome copies of AAV:Control-shRNA or AAV:GADD34-shRNA. The clinical phenotype and pathology were characterized as described below.

Assessment of clinical phenotype

Mice were weighed three times a week and clinically assessed for weakness, as previously described (Boillee et al., 2006). The onset of disease was defined as peak weight before beginning of loss of weight; early phase of disease was the time from onset until loss of 10% of peak weight; and late phase of disease was the time from 10% weight loss until end stage when a mouse was unable to right itself within 20 seconds after being put on its back. In some experiments, non-transgenic littermate mice were used as additional controls.

G85R-SOD1 mouse pathology following GADD34 shRNA knockdown

G85R-SOD1 mice that had been uninjected or injected as neonates with either AAV:Control-shRNA or AAV:GADD34-shRNA and sacrificed at two different times: ~355 days (which was end stage for untreated and Control-shRNA-treated G85R-SOD1 mice) and ~390 days (which was end stage for GADD34-shRNA-treated G85R-SOD1 mice). Anesthetized mice were perfused transcardially using cold phosphate buffered saline (PBS) followed by 4% paraformaldehyde. At least eight to 12 sections of the anterior horn of both the cervical and lumbar spinal cord from each of 3-5 G85R-SOD1 mice were processed for pathological evaluation.

Nissl staining was performed to assess numbers of motor neurons (i.e., cells larger than 18.5 μM in size). The area of diffuse and punctate staining of SOD1 as well as the number of SOD1 aggregates (equivalent to the number of SOD1-positive punctates) were identified by immunofluorescent studies using a rabbit antibody that recognizes the carboxyl end of mouse and human SOD1 [1:3000 dilution, (Deng et al., 2006)], and then Alexa Fluor 594 goat anti-rabbit secondary antibody (1:1000 dilution, Invitrogen) as previously described (Ghadge et al., 2019). Reactive microglia and astrocytes were detected by using rabbit anti-IbaI (ionized calcium-binding adaptor molecule 1, 1:1000 dilution, Wako, Richmond, VA) and mouse anti-GFAP (glial fibrillary acid protein, 1:1000 dilution, Chemicon, Temecula, CA) antibodies respectively, followed by either anti-rabbit or anti-mouse horseradish peroxidase (ImmPRESS Reagents, Vector Labs, Burlingame, CA) according to the manufacturer's instructions.

Imaging was performed at the University of Chicago Integrated Light Microscopy Facility. Digital image files were created with a 3D Histech Pannoramic Scan whole slide scanner (Perkin Elmer, Waltham, MA) with a Zeiss AxioCam MRm CCD camera (fluorescence images, Carl Zeiss Microscopy, Thornwood, NY) or 2M pixel 3CCD CIS camera (histology images, Daitron Co., LTD., Fukuoka, Japan). Individual images were created with the 3D Histech Pannoramic Viewer software (Perkin Elmer, Waltham, MA). Quantification of motor neurons, SOD1 aggregates, astrocytosis, and microgliosis was performed using ImageJ software, and presented as mean +/- standard error mean (SEM). The background was subtracted and threshold was automated using the Otsu method embedded in the ImageJ program. The percent area of SOD1 load, GFAP- and IbaI–staining, and counts of motor neurons and mtSOD1 aggregates were calculated using standard features of ImageJ.

Extraction of RNA and protein from spinal cords

In some experiments, spinal cords were dissected following perfusion of mice with cold PBS, then placed in 1 ml TRIzol, and homogenized by passing it through a syringe with a 23G needle 10 times. RNA and protein extraction was performed according to the manufacturer's protocol except that the precipitated protein was solubilized by adding a 1:1 solution of 8 M urea in 1 M Tris-HCl, pH8.0 and 1% SDS containing a protease inhibitor and phosphatase inhibitor cocktail followed by sonication, as described previously (Simoes et al., 2013).

RT-PCR

RNA from NSC-34 cells was treated with DNase I (Invitrogen) for 30 min at 37°C, and then extracted using RNeasy Mini kit (Qiagen, Germantown, MD). Reverse transcription was performed using SuperScript III First-Strand Synthesis System (Appliedbiosystems, Pleasanton, CA). Quantitative PCR was performed by Taqman Real-time PCR Assays (GADD34, Mm01205601_g1; HPRT, Mm01545399_m1; β-actin, Mm00607939_s1; CHOP, Mm01135937_g1) using Taqman Gene Expression Master Mix (AppliedBiosystems) or SYBR Green Real-time PCR Assays. The forward (F) and reverse (R) primers using Power SYBR Green PCR Master Mix (AppliedBiosystems) in a CFX96 Real-Time System (BIO-RAD, Hercules, CA) were: GFP-F, CAAAGACCCCAACGAGAAGC; GFP-R, CTTGTACAGCTCGTCCATGC; β-actin-F, GGCTGTATTCCCCTCCATCG and β-actin-R, CCAGTTGGTAACAATGCCATGT.

Western blots

Five to 30 µg of total protein from spinal cord or NSC-34 cell lysates were subjected to electrophoresis on 8.5%, 12.5%, or 15% SDS polyacrylamide gels, and then transferred to Amersham Hybond P 0.45 µm PVDF membrane (GE Healthcare, Marlborough, MA). The membrane was first blocked with 1% non-fat skim milk in Tris-buffered saline (50 mM Tris-HCL, pH 7.4, 150 mM NaCL) containing 0.05% Tween-20 for 1h at room temperature, and then overlaid overnight at 4°C with primary antibodies against CHOP (1:1000, D46F1, Cell Signaling Technology), GADD34 (1:200, C-19, Santa Cruz Biotechnology, Dallas, TX), β-actin (1:5000, AC-15, MilliporeSigma), p-eIF2α (1:1000, 119A11, Cell Signaling Technology, Danvers, MA), eIF2α (1:1000, D7D3, Cell Signaling Technology), or GFP (1:1000, D5.1, Cell Signaling Technology). Finally the membrane was incubated with anti-mouse or anti-rabbit horseradish peroxidase–conjugated secondary antibodies (1:5000, GE Healthcare) for 1 h at room temperature. The signals were detected using SuperSignal West Dura Extended Duration

Substrate (Thermo Fisher Scientific, Rockford, IL) and analyzed using ChemiGenius2 (Syngene) or ChemiDoc MP Imaging System (BIO-RAD).

Global translation was assessed as previously published (Goodman et al., 2011; Schmidt et al., 2009). In brief, 5 µg/ml of puromycin was added to NSC-34 cells following treatment with thapsigargin, and cells were then cultured for 30 min. The protein was extracted, and Western blots were immunostained with antibody against puromycin (1:1000, 12D10, MilliporeSigma). After the blots were stripped with Restore PLUS Western Blot Stripping Buffer (Thermo Fisher Scientific), staining with Coomassie Blue was carried out to ensure equal loading of proteins. The puromycin-labeled and Coomassie Blue-stained protein signals were analyzed by densitometric measurement of whole lanes using a ChemiDoc MP Imaging System (BIO-RAD), and quantitated with ImageJ software. Global translation was calculated as the ratio of puromycin-labeled protein signal to the Coomassie Blue−stained protein signal. All sample signals were normalized to the thapsigargin-treated Control-shRNA sample.

Western blots to assess CHOP protein knockdown in the central nervous system was carried out on spinal cord lysates using rabbit anti-CHOP monoclonal antibody, D46F1 (Cell Signaling Technology) followed by anti-rabbit horseradish peroxidase–conjugated secondary antibodies (1:5000, GE Healthcare).

Statistics

The data was statistically analyzed with GraphPad Prism 7 software. Sidak's or Tukey multiple comparison test was used to determine statistical significance following one-way ANOVA analysis. The log-rank (Mantel-Cox) test was used to calculate statistical significance following survival analysis.

Journal Pre-proof

Results

An ASO that knocks down CHOP does not ameliorate disease in G93A and G85R mtSOD1 mice

In order to select an ASO that suppresses CHOP expression effectively, wild type mice were i.c.v. injected with CHOP ASOs as well as a control ASO followed two weeks later by an i.c.v. injection of tunicamycin to induce ER stress. RT-PCR of lysates of spinal cords harvested 3 days after the tunicamycin injection showed that ASOs 1, 2, 3, and 4 significantly suppressed tunicamycin-induced expression of CHOP mRNA compared to control ASO- or PBS-injected mice ($P < 0.0001$) (Fig. 1A). Western blots showed that ASO2 suppressed tunicamycin-induced expression of CHOP protein by over 80% compared to tunicamycin-treated control ASO- or PBS-injected mice ($P < 0.001$) (Fig. 1B).

Survival assays of mtSOD1 transgenic mice were carried out using ASO2 since this ASO had the most prominent knockdown of CHOP on Western blots (Fig. 1B). We injected ASO2 i.c.v. into G93A-SOD1 mice at both 75 and 105 days of age, and into G85R-SOD1 mice at 250 days of age. Compared to PBS and control ASO, CHOP ASO2 led to no significant change in G93A-SOD1 mice in disease onset (PBS-treated, mean of 118+/-2.1 days; control ASO-treated, mean of 112+/-2.3 days; CHOP ASO2-treated, mean of 112+/-3.2 days [$p>0.05$, Fig. 1C]) or survival (PBS-treated, mean of 156+/-1.2 days; control ASO-treated, mean of 154+/-1.7 days; CHOP ASO2-treated, mean of 153+/-0.9 days [$p>0.05$, Fig. 1D]). Similarly, compared to PBS and control ASO, ASO2 led to no change in G85R-SOD1 mice in disease onset (PBS-treated, mean of 301+/-7.6 days; control ASO-treated, 288+/-9.0 days; CHOP ASO2-treated, 316+/-11.6 days [$p>0.05$, Fig. 1E]) or survival (PBS-treated, mean of 345+/-7.2 days; control ASO-treated, 334+/-11.6 days; CHOP ASO2-treated, 350+/-13.6 days [$p>0.05$, Fig. 1F]). These results suggest that knockdown of CHOP does not affect survival of mtSOD1 mice.

GADD34 shRNA knocks down GADD34

Our previous studies demonstrated the importance of the UPR/ISR in perturbing mtSOD1-induced disease (Wang et al., 2011; Wang et al., 2014a; Wang et al., 2014b). We were unable to identify an ASO that efficiently knocked down GADD34, and therefore investigated knockdown of GADD34 with shRNAs. We first tested the effect of GADD34-shRNA-55 and GADD34-shRNA expression *in vitro*. NSC-34 cells were transfected with pFB plasmids expressing Control-shRNA or GADD34 shRNA, and 48 hours later treated with 500 nM thapsigargin to trigger ER stress. The cells were processed 24 hours later for RT-PCR, Western blotting, and an assay of global translation. Figure 2A, B shows a statistically significant knockdown of GADD34 mRNA and protein following thapsigargin administration by GADD34-shRNA-55 and GADD34-shRNA. As expected, GADD34-shRNA was more efficient than GADD34-shRNA-55 in downregulating expression of GADD34. The GADD34-shRNA led to a decrease in GADD34 protein levels (Fig. 2C, D) and an increase in the level of p-eIF2α (Fig. 2C, E), resulting in a statistically significant block in global protein translation (Fig. 2F).

We then tested the effect of AAV9-encoded GADD34-shRNA-55 and GADD34-shRNA in wild type C57BL/6J mice under ER stress. Mice were injected in the temporal vein as neonates with AAV:Control-shRNA, AAV:GADD34-shRNA-55, or AAV:GADD34-shRNA,

and then 81 days later injected with tunicamycin in the lateral ventricle to trigger ER stress, and finally sacrificed 3 days later. Following tunicamycin treatment, there was a statistically significant decrease in GADD34 mRNA in spinal cord homogenates of mice that had been injected as neonates with AAV:GADD34-shRNA compared to mice that had been injected with AAV:Control-shRNA (Fig. 3A, $p<0.01$). The decrease in GADD34 mRNA following the AAV:GADD34-shRNA knockdown was relatively modest (but statistically significant), presumably because the shRNA is preferentially delivered to motor neurons after the neonatal intravenous injection of AAV (Foust et al., 2009; Foust et al., 2013), whereas all neural cells have GADD34 upregulation from thapsigargin. In this way, a dilution effect from the upregulation of GADD34 in non-motor neural cells could mask the actual knockdown in motor neurons. This dilution effect could explain the statistically insignificant decrease in GADD34 mRNA following GADD34-shRNA-55 treatment (Fig. 3A). Of note, there was an increase in GADD34 mRNA in mice that received tunicamycin and shRNA compared to those that just received tunicamycin (labelled as "untreated", Fig. 3A), suggesting that the virus vector delivery and expression of shRNA and GFP increased ER stress.

The amount of GFP mRNA was similar in the spinal cord of mice that received the AAV:Control-shRNA and those that received AAV:GADD34-shRNA (Fig. 3B, $p>0.05$), suggesting that there had been no increase in death of cells that received the AAV:GADD34-shRNA over cells that had just received AAV:Control-shRNA. Furthermore, there was no clinical or pathological evidence of any toxicity in the injected mice.

To determine whether the GADD34 knockdown in these mice influences translation, we immunostained electrophoresed spinal cord lysates from mice with anti-GFP antibody since GFP was expressed along with the shRNA. The results showed that although there were similar amounts of GFP mRNA in mice that received AAV:Control-shRNA and those that received AAV:GADD34-shRNA, there was abundant GFP protein expression in mice that received AAV:Control-shRNA, but little GFP protein in mice that received AAV:GADD34-shRNA ($p<0.0001$, Fig. 3C). These results suggested that cells that received the GADD34-shRNA had a more sustained eIF2α phosphorylation, leading to a block in translation and decreased GFP protein synthesis compared to cells from other mice that just received Control-shRNA. GADD34-shRNA-55 treatment showed a block in translation of GFP protein similar to that seen with GADD34-shRNA ($p<0.0001$, Fig. 3C).

AAV:GADD34-shRNA injection of neonatal G93A and G85R mtSOD1 mice, but not adult G93A mtSOD1 mice, ameliorates disease

In order to test the effect of GADD34 knockdown on disease in mtSOD1 mice, we selected GADD34-shRNA for mouse experiments since it had a robust knockdown of GADD34 mRNA and protein *in vitro* and in mice than GADD34-shRNA-55 (Figs. 2, 3). An AAV was prepared that encoded GADD34-shRNA.

We first carried out studies on G93A-SOD1 mice injected as neonates (P1). These mice were injected in the temporal vein with $5X10^{11}$ viral genome copies of either AAV:Control-shRNA or AAV:GADD34-shRNA; untreated G93A-SOD1 mice were used as an additional control. There was no significant difference in the onset of disease among the three groups of

G93A-SOD1 mice: untreated (n=16, mean of 122+/-2.6 days), Control-shRNA-treated (n=12, 119+/-2.0 days), and GADD34-shRNA-treated (n=19, 119+/-2.4 days) ($p>0.05$, Fig. 4A); however, GADD34-shRNA-treated G93A-SOD1 mice had a significantly increased survival (n=17, mean of 179+/-2.0 days) compared to mice treated with Control-shRNA (n=11, 166+/-2.0 days) or no treatment (n=16, 164+/-1.9 days) ($p<0.0001$, Fig. 4B). The early phase of disease (i.e., the period between peak weight and 10% weight loss) was statistically similar for GADD34-shRNA-treated (30+/-2.5 days), Control-shRNA-treated (31+/-2.8 days), and untreated (24+/-2.0 days) G93A-SOD1 mice ($p>0.05$, Fig. 4C); however, the late phase of the disease (i.e., the period from 10% weight loss to end stage) of G93A-SOD1 mice was significantly longer for GADD34-shRNA-treated (30+/-2.4 days) when compared to Control-shRNA-treated (17+/-1.6 days) or untreated (17+/-1.7 days) mice ($p<0.001$ or $p<0.0001$ respectively, Fig. 4D).

We carried out similar studies with neonatal-treated G85R mtSOD1 mice. The three groups of G85R mice, like the G93A mice, failed to show a difference in disease onset: untreated (n=7, 285+/-9.5 days), Control-shRNA-treated (n=11, 283+/-4.3 days), and GADD34-shRNA-treated (n=12, 283+/-5.2 days) ($p>0.05$, Fig. 5A); however, G85R-SOD1 mice treated with GADD34-shRNA showed an increase in survival (n=9, 386+/-6.3 days) compared to mice treated with Control-shRNA (n=13, 337+/-10.4 days) or untreated mice (n=8, 340+/-13.0 days) ($p<0.001$, Fig. 5B). There was no statistically significant difference in the early phase of disease among three groups of G85R-SOD1 mice: GADD34-shRNA-treated (62+/-2.7 days), Control-shRNA-treated (49+/-4.2 days), and untreated (52+/-7.6 days) ($p>0.05$, Fig. 5C); however, GADD34-shRNA treated G85R-SOD1 mice had a significant prolongation in the late phase of disease similar to that seen in GADD34-shRNA-treated G93A-SOD1 mice: GADD34-shRNA-treated (33+/-4.2 days) , Control-shRNA-treated (19+/-1.7 days) and untreated (11+/-1.6 days) ($p<0.01$ or $p<0.001$ respectively, Fig. 5D). The difference in the late phase of disease between Control-shRNA-treated and untreated G85R-SOD1 mice was not statistically significant ($p>0.05$).

In contrast to the above results that showed an extension of survival following neonatal injections of AAV:GADD34-shRNA into G93A and G85R mtSOD1 mice, a tail vein injection of G93A-SOD1 mice treated at ~120 days failed to change disease onset or survival. Onset of the disease was similar in G93A-SOD1 mice treated with GADD34-shRNA (n=18, 123+/-1.1 days) compared to untreated mice (n=11, 122+/-2.3 days) or Control-shRNA-treated mice (n=19, 124+/-1.0 days) ($p>0.05$, Fig. 6A). Similarly AAV:GADD34-shRNA injection at ~120 days showed no effect on survival (160+/-1.8 days) compared to untreated mice (160+/-2.1 days) and Control-shRNA-treated mice (166+/-2.3 days) ($p>0.05$, Fig. 6B).

Neonatal injection of G85R-SOD1 mice with AAV:GADD34-shRNA leads to a decrease in pathology

The anterior horn of the cervical and lumbar spinal cords of G85R-SOD1 mice treated as neonates with GADD34-shRNA was examined for mtSOD1 load and the number of aggregates. At the age of ~355 days, G85R-SOD1 mice that had been treated with GADD34-shRNA as neonates showed a decreased area of mtSOD1-positivity compared to Control-shRNA-treated (cervical, $p<0.0001$; lumbar, $p<0.01$) and untreated G85R-SOD1 mice (cervical and lumbar, $p<0.0001$) (Fig. 7A, B). There was also significantly less SOD1 aggregation in the cervical and

lumbar spinal cord of GADD34-shRNA-treated G85R-SOD1 mice compared to untreated and Control-shRNA-treated mice ($p<0.0001$) (Fig. 7A, C). These observations suggest that the block in translation from the GADD34 knockdown decreased the amount of mtSOD1 that is synthesized. By end stage (~390 days), the mtSOD1 load increased, but was not statistically significant different when compared to results at ~355 days (cervical and lumbar, $p>0.05$) (Fig. 7A, B). On the other hand, mtSOD1 aggregation in the GADD34-shRNA-treated G85R-SOD1 mice at ~390 days was statistically significant when compared to the results at ~355 days (cervical, $p<0.001$; lumbar, $p<0.0001$) (Fig. 7A, C).

In order to determine the effect of GADD34-shRNA on pathology of G85R-SOD1 mice treated as neonates, we examined the anterior horn of both lumbar and cervical spinal cord. At ~355 days of age, GADD34-shRNA-treated G85R-SOD1 mice demonstrated a relative preservation of motor neurons as assessed by a greater number of Nissl-stained cells (Fig. 8A top panel, 8B), when compared to untreated and Control-shRNA-treated G85R-SOD1 mice. In addition, there was less astrocytosis, as assessed by fewer GFAP-positive cells (Fig. 8A middle panel, 8C), and less microgliosis, as assessed by fewer Iba1-positive cells (Fig. 8A bottom panel, 8D) than untreated and Control-shRNA-treated G85R-SOD1 mice. However, at end stage (~390 days), GADD34-shRNA-treated G85R-SOD1 mice showed a loss of motor neurons and astrocytosis and microgliosis similar to that seen in end stage untreated or Control-shRNA-treated G85R-SOD1 mice. In summary, GADD34-shRNA treatment delayed pathology of G85R-SOD1 mice.

Journal Pre-proof

Discussion

Despite the recognition of ALS for over a century and despite the identification of mutations in a number of different genes that cause FALS, treatments for this progressive and fatal disease are suboptimal. In the case of mtSOD1-caused FALS, the mutant protein leads to a plethora of gain of function negative effects, especially related to the mutant protein's misfolding (Taylor et al., 2016). Of note, misfolded proteins are not only present in mtSOD1-induced ALS, but also in sporadic ALS (and other neurodegenerative diseases) as well. In the present study, we targeted mtSOD1 misfolding by knocking down CHOP, a proapoptotic gene downstream of the UPR/ISR, and GADD34.

One way in which cells respond to the presence of misfolded proteins in the ER is through the UPR/ISR. A number of studies have found activation of the UPR/ISR in ALS (reviewed in (Medinas et al., 2017)). For example, PERK and downstream pathways reactive to ER stress have been found to be activated very early in motor neurons of G93A mice, perhaps at least partly because of low levels of ER chaperones in these cells (Sun et al., 2015). In addition, laser-captured motor neurons of G37R mice showed a prominent upregulation of ATF4 and CHOP expression (Sun et al., 2015). Using a genetic approach we previously found that: i) G85R-SOD1 mice that are PERK haploinsufficient (and have a less sustained UPR) have a significantly shorter survival compared to G85R SOD1 mice with wild type levels of PERK (Wang et al., 2011), ii) G85R-SOD1 mice with a mutant GADD34 (and have a more sustained UPR) have an increased survival as compared to G85R-SOD1 mice with wild type levels of GADD34 (Wang et al., 2014a). In addition, treatment with a number of drugs that enhance the UPR/ISR have been found to ameliorate disease in G93A-SOD1 mice (Jiang et al., 2014; Saxena et al., 2009; Wang et al., 2014b); however, the targets of some of these drugs have been called into question (Crespillo-Casado et al., 2017) and the results with one drug were unable to be confirmed (Vieira et al., 2015). Furthermore, a recent study using a genetic approach found that the PERK/UPR pathway was not a promising therapeutic target (Dzhashiashvili et al., 2019). Importantly, different results from a drug intervention (as in our study) vs. a genetic knockdown or knockout have been documented before, perhaps related at least partly because of the use of redundant pathways when genes are knocked down or out (Knight and Shokat, 2007).

The above results, although somewhat mixed, prompted us to investigate reagents that target the UPR/ISR and could be adapted for use in patients with mtSOD1-induced FALS. In the present study, we made use of an ASO to knockdown CHOP and AAV9-delivered GADD34 shRNA to reduce GADD34 expression.

We found no change in survival of G93A and G85R mtSOD1 mice that were injected i.c.v. with a CHOP ASO. These negative results may suggest that CHOP is not a key factor in disease pathogenesis in G93A and G85R mice, perhaps because other apoptotic genes are active when the UPR/ISR is overwhelmed. On the other hand, it may be that the timing of the ASO injection was not an optimal one, especially in the case of the G85R mouse, since the activity of ASO is somewhat limited. For this reason, additional injections in the G85R mouse might be necessary in order to see an effect on survival. Furthermore, it may be that an effect on survival would have been apparent if a larger number of mice had been used.

In contrast to the above negative results, we found that G93A and G85R mice that received AAV:GADD34-shRNA as neonates exhibited a significantly increased lifespan compared to untreated and AAV:Control-shRNA-treated mtSOD1 mice. In addition, the G85R mice treated as neonates with AAV:GADD34-shRNA exhibited less motor neuron death, decreased astrocytosis and decreased microgliosis compared to untreated and Control-shRNA-treated mtSOD1 mice. We also found a reduced mtSOD1 aggregation and load, presumably because the knockdown of GADD34 in motor neurons led to a decrease in translation as a result of a more sustained eIF2α phosphorylation (Jiang et al., 2014; Vieira et al., 2015; Wang et al., 2014a; Wang et al., 2014b). This reduction in mtSOD1 aggregation and load may have led to the decreased motor neuron death as well as decreased glial cell response.

The impact of AAV:GADD34-shRNA on disease was much more significant in the case of G85R mice when compared to G93A mice. These varying effects may have been observed because different mutant SOD1s lead to disease in different ways. The lesser effect of the GADD34 knockdown in G93A mice might have resulted from the very aggressive disease manifest by G93A mice. In addition, the extensive mtSOD1 aggregation seen in G85R mice (Bruijn et al., 1997; Wang et al., 2002) may make this transgenic mouse more liable to exhibit disease amelioration with an enhancement of the UPR/ISR. It is important to note that in some ways the G85R mice may be a better model of human ALS because both have a slow course.

We failed to have an impact on disease when ~120 day-old G93A-SOD1 mice were injected with AAV:GADD34-shRNA, which is unfortunate since ALS is a disease of adult patients. There are several possible reasons for this failure including: i) the burden of misfolded proteins in adult G93A-SOD1 mice may have been too great to be overcome - and far greater than in neonatal mice; ii) while AAV9 intravenous injection of neonates targets the motor neuron, AAV9 intravenous injection of adults delivers the transgene primarily to glial cells (Foust et al., 2009; Foust et al., 2013). In future studies, it may be valuable to use other AAV serotypes that have a different species specificity, CNS tropism, or ability to cross the blood brain barrier (Deverman et al., 2016; Hordeaux et al., 2018), and to inject intracerebroventricularly, which may allow for a more broad neural cell type tropism.

The present findings are significant because they emphasize the importance of the UPR/ISR in ALS pathogenesis, and the possibility of targeting the UPR/ISR in treating ALS. The results also suggest that targeting the UPR/ISR could be applicable to a number of other neurodegenerative diseases in which misfolded proteins and ER stress have been implicated. However, it is important to note that the UPR/ISR affects many genes, including some that do not target unfolded proteins. For example, GADD34 plays a role in cytokine production and the host immune response (Clavarino et al., 2012a; Clavarino et al., 2012b; Dalet et al., 2017; Kavaliauskis et al., 2016; Liebermann and Hoffman, 2002), and may have a direct role in the innate immune response (Mesman et al., 2014). Also, of concern is the observation that enhancing the UPR/ISR may have deleterious effects by leading to expression of apoptotic genes, resulting in cell death. For this reason, the timing of enhancing the UPR/ISR is important in the outcome, and at some point suppressing the UPR may be advantageous (Kim et al., 2014).

In summary, the current study demonstrates the efficacy of treating mtSOD1 transgenic mice by targeting GADD34, a key enzyme in the UPR/ISR; however, the results only showed

efficacy when mtSOD1 mice were treated as neonates. The results suggest that earlier treatment of mutant gene-induced FALS is most effective, and that successful treatment of adults with GADD34 shRNA may require new AAV serotypes and intracerebroventricular injections.

Journal Pre-proof

Figure Legends

Fig. 1. Knockdown of CHOP does not affect disease course of both G93A-SOD1 and G85R-SOD1 mice. (A, B) PBS, control (Con) ASO or CHOP ASOs (ASOs 1-5) were injected i.c.v. into wild type mice. Fourteen days later, tunicamycin or DMSO was injected i.c.v. into the same mice. The spinal cords were collected 3 days later to assess levels of (A) CHOP mRNA by RT-PCR, and (B) protein by Western blot: a representative Western blot is shown in the upper panel and a bar diagram showing quantification of Western blots from the spinal cords of 3 mice is shown below. (C) Onset and (D) survival curves of G93A-SOD1 mice that were injected i.c.v. with PBS (n=16), control ASO (n=16) or CHOP ASO2 (n=16) at both 75 and 105 days of age. (E) Onset and (F) survival curves of G85R-SOD mice that were injected i.c.v. with PBS (n=7), control ASO (n=9) or CHOP ASO 2 (n=6) at 250 days of age. Sidak's multiple comparison test was used to determine statistical significance following one-way ANOVA analysis of A and B and the bar graphs in Figures 2, 4-8. The log-rank (Mantel-Cox) test was used to calculate statistical significance following survival analysis of C-F, and the following figures. ** = $p<0.01$, *** = $p<0.001$, **** = $p<0.0001$.

Fig. 2. GADD34 shRNA decreases expression of GADD34, increases phosphorylation of eIF2α and blocks translation in cultured cells. NSC-34 cells were transfected with pFB plasmids encoding Control-shRNA, GADD34-shRNA-55 or GADD34-shRNA. Forty-eight hours later, the cells were treated with thapsigargin for either 24 hours or as indicated to induce ER stress. Quantification of three experiments showed that compared to Control-shRNA-transfected cells GADD34 shRNAs decreased (A) GADD34 mRNA ($p<0.0001$) and (B) protein (GADD34-shRNA, $p<0.0001$; GADD34-shRNA-55, $p>0.05$). (C) Representative Western blot of NSC-34 cells lysed at varying times after thapsigargin administration showing decreased GADD34 protein levels and increasing eIF2α phosphorylation following GADD34-shRNA expression. (D) Quantification of GADD34 protein on Western blots from three experiments shows a statistically significant decreased expression at 8 and 24 hours thapsigargin treatment ($p<0.0001$). (E) Quantification of p-eIF2α on Western blots from three experiments shows a significant increase at 8 hours after thapsigargin treatment (* = $p<0.05$). (F) Quantitative analysis of Western blot of lysates from thapsigargin-treated NSC-34 cells shows a decrease in protein translation as indicated by the statistically significant decline in the ratio of puromycin-labeled proteins to Coomassie Blue–stained proteins following GADD34-shRNA expression compared to Control-shRNA expression ($p<0.01$). Sample signals were normalized to the thapsigargin-treated Control-shRNA sample. Con = control, GAD = GADD34, TG = thapsigargin. * = $p<0.05$, ** = $p<0.01$, **** = $p<0.001$.

Fig. 3. GADD34 shRNA decreases GADD34 and protein translation in the spinal cord of ER-stressed mice. C57BL/6 mice were injected in the temporal vein as neonates with AAV:Control-shRNA, AAV:GADD34-shRNA-55, or AAV:GADD34-shRNA, and then 81 days later injected i.c.v. with tunicamycin in the lateral ventricle. Mice were sacrificed 3 days later, and spinal cord lysates were subjected to RT-PCR and Western blotting. (A) GADD34 mRNA levels were reduced following GADD34-shRNA treatment compared to Control-shRNA treatment ($p<0.01$). (B) GFP mRNA levels were similar in the spinal cord lysates of mice treated with Control-shRNA and GADD34-shRNA ($p>0.05$). (C) Top panel: Representative Western blot of spinal cord lysates showing prominent GFP immunoreactivity following infection of mice with

AAV:Control-shRNA, but little GFP immunoreactivity following injection with AAV:GADD34-shRNA-55 and AAV:GADD34-shRNA. Bottom panel: Bar diagram showing quantification of Western blot results from 3 mice. Tukey's multiple comparison test was used to calculate statistical significance following one-way ANOVA analysis.
NS = not significant, ** = $p<0.01$, **** = $p<0.0001$.

Fig. 4. G93A-SOD1 mice survived longer and showed a more prolonged late phase of disease when injected as neonates with AAV:GADD34-shRNA than when uninjected or when injected with AAV:Control-shRNA. (A) There was no significant difference in the timing of the onset of disease between three groups of G93A-SOD1 mice that were untreated (n=16) or treated with Control-shRNA (n=12) or GADD34-shRNA (n=19). (B)There was a significant increase in survival of G93A-SOD1 mice treated with GADD34-shRNA (n=17) as compared to mice either untreated (n=16) or treated with Control-shRNA (n=11) ($p<0.0001$). There was no change in the (C) early phase of disease, but there was a prolongation in the (D) late phase of disease. *** = $p<0.001$, **** = $p<0.0001$.

Fig. 5. G85R-SOD1 mice survived longer and showed a more prolonged late phase of disease when injected as neonates with AAV:GADD34-shRNA compared to untreated or when injected with AAV:Control-shRNA. (A) There was no significant difference in the onset of disease among G85R-SOD1 mice that were untreated (n=7) or treated with Control-shRNA (n=11) or GADD34-shRNA (n=12). (B) There was a significant increase in survival of G85R-SOD1 mice treated with GADD34-shRNA (n=9) when compared to either untreated mice (n=8) or mice treated with Control-shRNA (n=13) ($p<0.001$). There was no change in the (C) early phase of disease, but there was a prolongation in the (D) late phase of disease. ** = $p<0.01$, *** = $p<0.001$.

Fig. 6. G93A-SOD1 mice injected intravenously at ~120 days of age with AAV:GADD34-shRNA (n=18) led to a similar (A) disease onset and (B) survival when compared to untreated mice (n=11) or mice injected with AAV:Control-shRNA (n=19) ($p>0.05$).

Fig. 7. AAV:GADD34-shRNA injection of neonatal G85R-SOD1 mice decreases SOD1 aggregation and load in the spinal cord. (A) Representative microfluorographs of sections of the anterior horn of the cervical and lumbar spinal cord of G85R-SOD1 mice (treated as neonates with AAV:GADD34-shRNA) at ~355 days of age showing fewer anti-SOD1 positive aggregates compared to untreated and mice injected with AAV:Control-shRNA. (B) GADD34-shRNA-treated G85R-SOD1 mice showed a decreased SOD1-immunoreactive area compared to Control-shRNA-treated (cervical, $p<0.0001$; lumbar, $p<0.01$) and untreated G85R-SOD1 mice (cervical and lumbar, $p<0.0001$). Mutant SOD1 load increased substantially by end stage (~390 days), but was not statistically significant (cervical and lumbar, $p>0.05$). (C) Quantification of number of SOD1 aggregates in the cervical and lumbar spinal cord of AAV:GADD34-shRNA-injected G85R-SOD1 mice when compared to uninjected or AAV:Control-shRNA-injected mice. GADD34-shRNA reduced the number of aggregates in the spinal cord of G85R-SOD1 at ~355 days of age. The mutant SOD1 aggregate count rose significantly from ~355 to ~390 days (cervical, $p<0.001$; lumbar, $p<0.0001$). NS = not significant, ** = $p<0.01$, *** = $p<0.001$, **** = $p<0.0001$.

Fig. 8. AAV:GADD34-shRNA injection of neonatal G85R-SOD1 mice delays pathology. Sections of the spinal cord were stained with: Nissl for motor neurons, anti-GFAP antibody for astrocytes, and anti-Iba1 antibody for microglia. (A) Representative micrographs showing preserved motor neurons (top row), reduced astrocytosis (middle row) and reduced microgliosis (bottom row) in the anterior horn of the lumbar spinal cord of ~355 day old G85R mtSOD1 mice that were untreated or treated with AAV:Control-shRNA or AAV:GADD34-shRNA; sections from nontransgenic mice are shown as an additional control. Motor neuron loss, astrocytosis and microgliosis increased at ~390 days. (B-D) Bar graphs of stained cells in the anterior horn of the cervical and lumbar spinal cord: (B) number of Nissl-stained motor neurons (mean+/-SEM per anterior horn), (C) GFAP-stained astrocytes (mean percent area+/-SEM per anterior horn), and (D) IbaI-stained microglia (mean percent area+/-SEM per anterior horn). NS = not significant, * = $p<0.05$, ** = $p<0.01$, *** = $p<0.001$, **** = $p<0.0001$.

Journal Pre-proof

Journal Pre-proof

Acknowledgments
This work was supported by a grant from the ALS Association (FP068110-01-PR), Target ALS, and the Lohengrin Foundation.

Journal Pre-proof

References

Boillee, S., et al., 2006. Onset and progression in inherited ALS determined by motor neurons and microglia. Science. 312, 1389-92.

Bruijn, L. I., et al., 1997. ALS-linked SOD1 mutant G85R mediates damage to astrocytes and promotes rapidly progressive disease with SOD1-containing inclusions. Neuron. 18, 327-38.

Chen, C. M., et al., 2012. C/EBP homologous protein (CHOP) deficiency aggravates hippocampal cell apoptosis and impairs memory performance. PLoS One. 7, e40801.

Clavarino, G., et al., 2012a. Induction of GADD34 is necessary for dsRNA-dependent interferon-beta production and participates in the control of Chikungunya virus infection. PLoS Pathog. 8, e1002708.

Clavarino, G., et al., 2012b. Protein phosphatase 1 subunit Ppp1r15a/GADD34 regulates cytokine production in polyinosinic:polycytidylic acid-stimulated dendritic cells. Proc Natl Acad Sci U S A. 109, 3006-11.

Crespillo-Casado, A., et al., 2017. PPP1R15A-mediated dephosphorylation of eIF2alpha is unaffected by Sephin1 or Guanabenz. Elife. 6.

Dalet, A., et al., 2017. Protein synthesis inhibition and GADD34 control IFN-beta heterogeneous expression in response to dsRNA. EMBO J. 36, 761-782.

Deng, H. X., et al., 2006. Conversion to the amyotrophic lateral sclerosis phenotype is associated with intermolecular linked insoluble aggregates of SOD1 in mitochondria. Proc Natl Acad Sci U S A. 103, 7142-7. Epub 2006 Apr 24.

Deverman, B. E., et al., 2016. Cre-dependent selection yields AAV variants for widespread gene transfer to the adult brain. Nat Biotechnol. 34, 204-9.

Dzhashiashvili, Y., et al., 2019. The UPR-PERK pathway is not a promising therapeutic target for mutant SOD1-induced ALS. Neurobiol Dis.

Foust, K. D., et al., 2009. Intravascular AAV9 preferentially targets neonatal neurons and adult astrocytes. Nat Biotechnol. 27, 59-65. Epub 2008 Dec 21.

Foust, K. D., et al., 2013. Therapeutic AAV9-mediated suppression of mutant SOD1 slows disease progression and extends survival in models of inherited ALS. Mol Ther. 21, 2148-59.

Ghadge, G. D., et al., 2019. Single chain variable fragment antibodies directed against SOD1 ameliorate disease in mutant SOD1 transgenic mice. Neurobiol Dis. 121, 131-137.

Goodman, C. A., et al., 2011. Novel insights into the regulation of skeletal muscle protein synthesis as revealed by a new nonradioactive in vivo technique. FASEB J. 25, 1028-39.

Hinnebusch, A. G., et al., 2016. Translational control by 5'-untranslated regions of eukaryotic mRNAs. Science. 352, 1413-6.

Hordeaux, J., et al., 2018. The Neurotropic Properties of AAV-PHP.B Are Limited to C57BL/6J Mice. Mol Ther. 26, 664-668.

Jiang, H. Q., et al., 2014. Guanabenz delays the onset of disease symptoms, extends lifespan, improves motor performance and attenuates motor neuron loss in the SOD1 G93A mouse model of amyotrophic lateral sclerosis. Neuroscience. 277, 132-8.

Kavaliauskis, A., et al., 2016. Activation of unfolded protein response pathway during infectious salmon anemia virus (ISAV) infection in vitro an in vivo. Dev Comp Immunol. 54, 46-54.

Kikuchi, H., et al., 2006. Spinal cord endoplasmic reticulum stress associated with a microsomal accumulation of mutant superoxide dismutase-1 in an ALS model. Proc Natl Acad Sci U S A. 103, 6025-30. Epub 2006 Apr 4.

Kim, H. J., et al., 2014. Therapeutic modulation of eIF2alpha phosphorylation rescues TDP-43 toxicity in amyotrophic lateral sclerosis disease models. Nat Genet. 46, 152-60.

Knight, Z. A., Shokat, K. M., 2007. Chemical genetics: where genetics and pharmacology meet. Cell. 128, 425-30.

Liebermann, D. A., Hoffman, B., 2002. Myeloid differentiation (MyD)/growth arrest DNA damage (GADD) genes in tumor suppression, immunity and inflammation. Leukemia. 16, 527-41.

Ling, K. K., et al., 2018. Antisense-mediated reduction of EphA4 in the adult CNS does not improve the function of mice with amyotrophic lateral sclerosis. Neurobiol Dis. 114, 174-183.

Medinas, D. B., et al., 2017. Proteostasis disturbance in amyotrophic lateral sclerosis. Hum Mol Genet. 26, R91-R104.

Mesman, A. W., et al., 2014. Measles virus suppresses RIG-I-like receptor activation in dendritic cells via DC-SIGN-mediated inhibition of PP1 phosphatases. Cell Host Microbe. 16, 31-42.

Reid, D. W., et al., 2016. Complementary Roles of GADD34- and CReP-Containing Eukaryotic Initiation Factor 2alpha Phosphatases during the Unfolded Protein Response. Mol Cell Biol. 36, 1868-80.

Rigo, F., et al., 2014. Pharmacology of a central nervous system delivered 2'-O-methoxyethyl-modified survival of motor neuron splicing oligonucleotide in mice and nonhuman primates. J Pharmacol Exp Ther. 350, 46-55.

Ron, D., Walter, P., 2007. Signal integration in the endoplasmic reticulum unfolded protein response. Nat Rev Mol Cell Biol. 8, 519-29.

Saxena, S., et al., 2009. A role for motoneuron subtype-selective ER stress in disease manifestations of FALS mice. Nat Neurosci. 12, 627-36. Epub 2009 Mar 29.

Schmidt, E. K., et al., 2009. SUNSET, a nonradioactive method to monitor protein synthesis. Nat Methods. 6, 275-7.

Simoes, A. E., et al., 2013. Efficient recovery of proteins from multiple source samples after TRIzol((R)) or TRIzo ((R))LS RNA extraction and long-term storage. BMC Genomics. 14, 181.

Sun, S., et al., 2015. Translational profiling identifies a cascade of damage initiated in motor neurons and spreading to glia in mutant SOD1-mediated ALS. Proc Natl Acad Sci U S A. 112, E6993-7002.

Swayze, E. E., et al., 2007. Antisense oligonucleotides containing locked nucleic acid improve potency but cause significant hepatotoxicity in animals. Nucleic Acids Res. 35, 687-700.

Taylor, J. P., et al., 2016. Decoding ALS: from genes to mechanism. Nature. 539, 197-206.

Vieira, F. G., et al., 2015. Guanabenz Treatment Accelerates Disease in a Mutant SOD1 Mouse Model of ALS. PLoS One. 10, e0135570.

Walker, A. K., Atkin, J. D., 2011. Stress signaling from the endoplasmic reticulum: A central player in the pathogenesis of amyotrophic lateral sclerosis. IUBMB Life. 63, 754-63.

Wang, J., et al., 2002. High molecular weight complexes of mutant superoxide dismutase 1: age-dependent and tissue-specific accumulation. Neurobiol Dis. 9, 139-148.

Wang, L., et al., 2011. The unfolded protein response in familial amyotrophic lateral sclerosis. Hum Mol Genet. 20, 1008-15.

Wang, L., et al., 2014a. An enhanced integrated stress response ameliorates mutant SOD1-induced ALS. Hum Mol Genet. 23, 2629-38.

Wang, L., et al., 2014b. Guanabenz, which enhances the unfolded protein response, ameliorates mutant SOD1-induced amyotrophic lateral sclerosis. Neurobiol Dis. 71C, 317-324.

Wooley, C. M., et al., 2005. Gait analysis detects early changes in transgenic SOD1(G93A) mice. Muscle Nerve. 32, 43-50.

Journal Pre-proof

Table 1. Sequence of control and CHOP ASOs

ID	Sequences
Control ASO	CCTATAGGACTATCCAGGAA
ASO 1	GTTTCCTAGTTCTTCCTTGC
ASO 2	TAGATCCTTTCTAACTCCTC
ASO 3	CTAGATCCTTTCTAACTCCT
ASO 4	CTAGCCCCTCTCTAGATCCT
ASO 5	GATGCAATTTTTTATTTTTC

Highlights

- A knockdown of CHOP by an antisense oligonucleotide does not affect survival of mutant SOD1 mice
- A knockdown of GADD34 in neonatal mutant SOD1 mice by shRNA attenuates disease and delays pathology
- GADD34 shRNA treatment of adult mutant SOD1 mice does not affect survival of mutant SOD1 mice

Journal Pre-proof

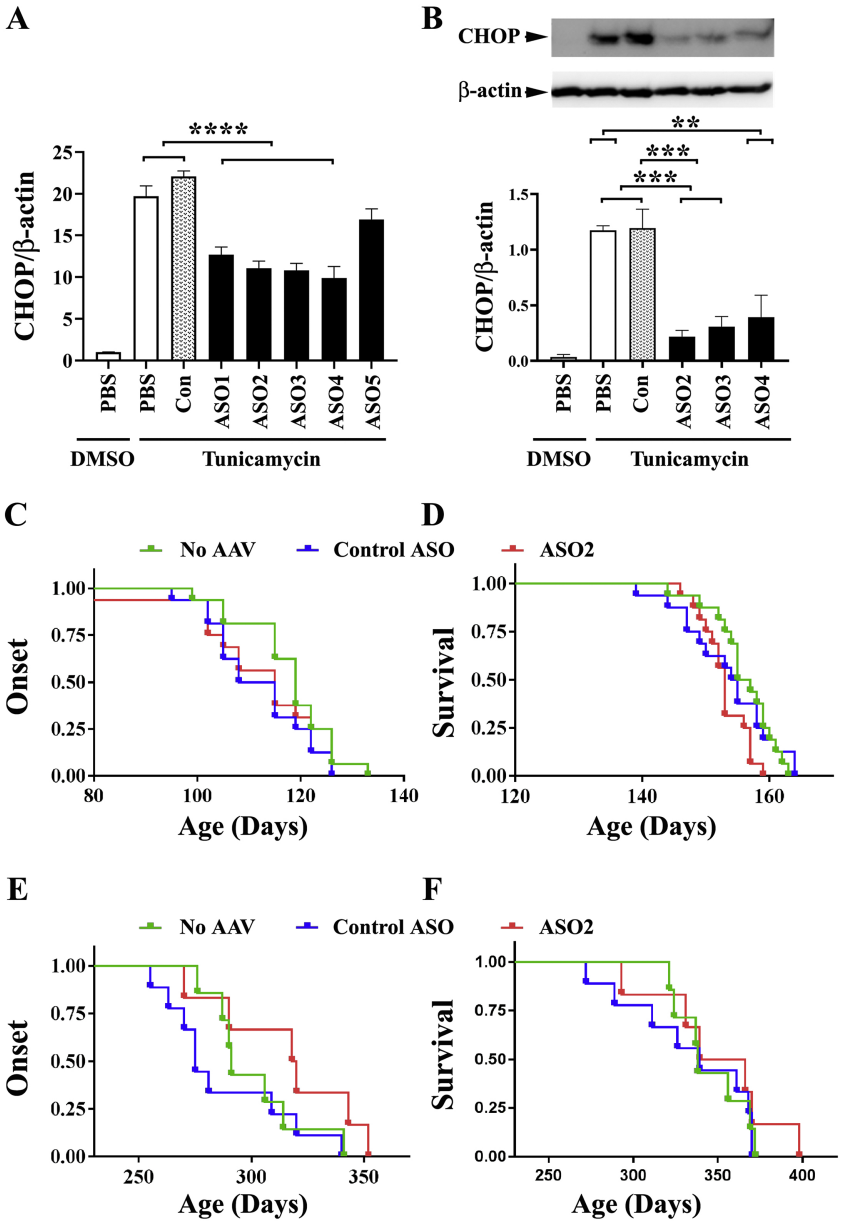
A
CHOP/β-actin
****
PBS
PBS
Con
ASO1
ASO2
ASO3
ASO4
ASO5
DMSO
Tunicamycin
B
CHOP
β-actin
**
***
***
CHOP/β-actin
PBS
PBS
Con
ASO2
ASO3
ASO4
DMSO
Tunicamycin
C
No AAV
Control ASO
Onset
Age (Days)
D
ASO2
Survival
Age (Days)
E
No AAV
Control ASO
Onset
Age (Days)
F
ASO2
Survival
Age (Days)

Figure 1

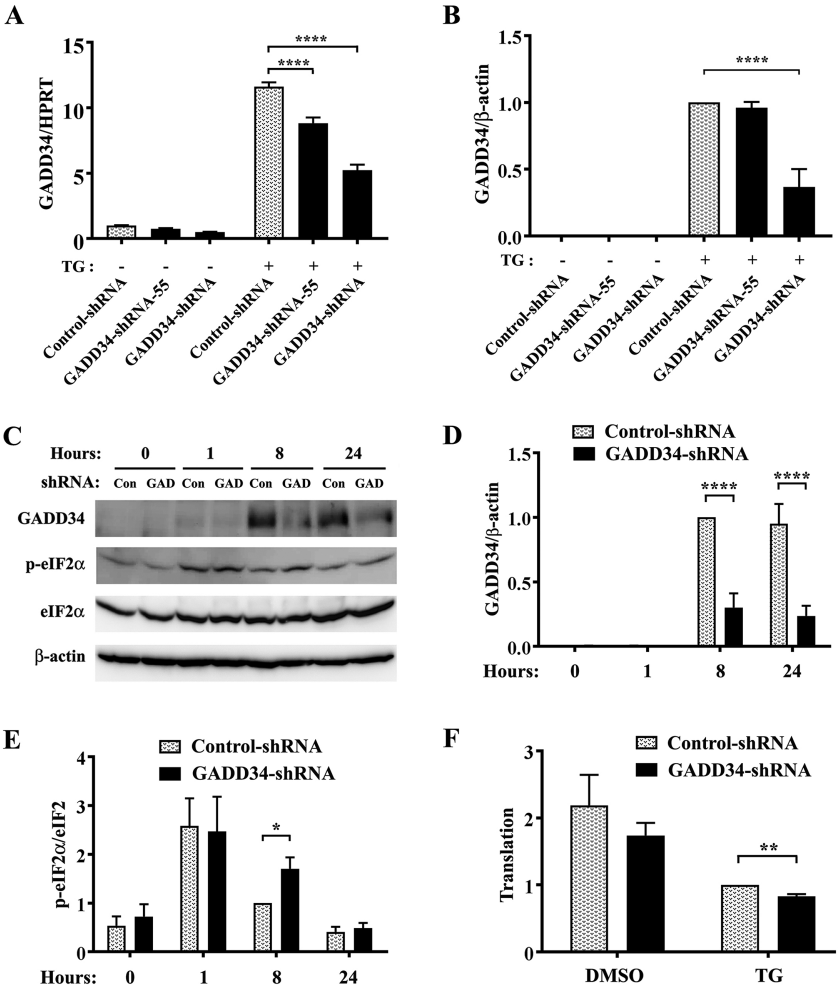
A
GADD34/HPRT
15
10
5
0
****
****
TG : - - - + + +
Control-shRNA
GADD34-shRNA-55
GADD34-shRNA
Control-shRNA
GADD34-shRNA-55
GADD34-shRNA
B
GADD34/β-actin
1.5
1.0
0.5
0.0
****
TG : - - - + + +
Control-shRNA
GADD34-shRNA-55
GADD34-shRNA
Control-shRNA
GADD34-shRNA-55
GADD34-shRNA
C
Hours: 0 1 8 24
shRNA: Con GAD Con GAD Con GAD Con GAD
GADD34
p-eIF2α
eIF2α
β-actin
D
Control-shRNA
GADD34-shRNA
GADD34/β-actin
1.5
1.0
0.5
0.0
****
****
Hours: 0 1 8 24
E
Control-shRNA
GADD34-shRNA
p-eIF2α/eIF2
4
3
2
1
0
*
Hours: 0 1 8 24
F
Control-shRNA
GADD34-shRNA
Translation
3
2
1
0
**
DMSO
TG

Figure 2

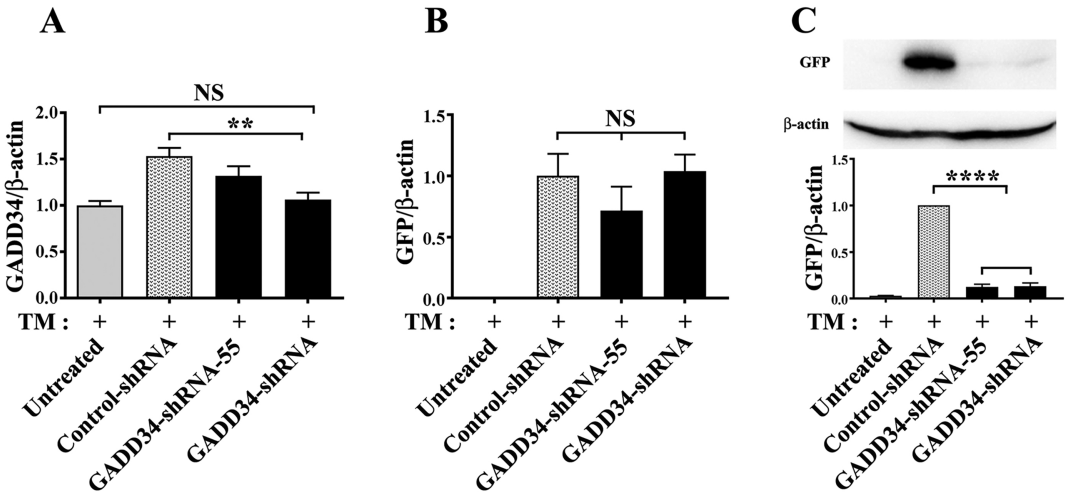
A
NS
**
GADD34/β-actin
2.0
1.5
1.0
0.5
0.0
TM : + + + +
Untreated
Control-shRNA
GADD34-shRNA-55
GADD34-shRNA
B
NS
GFP/β-actin
1.5
1.0
0.5
0.0
TM : + + + +
Untreated
Control-shRNA
GADD34-shRNA-55
GADD34-shRNA
C
GFP
β-actin
****
GFP/β-actin
1.5
1.0
0.5
0.0
TM : + + + +
Untreated
Control-shRNA
GADD34-shRNA-55
GADD34-shRNA

Figure 3

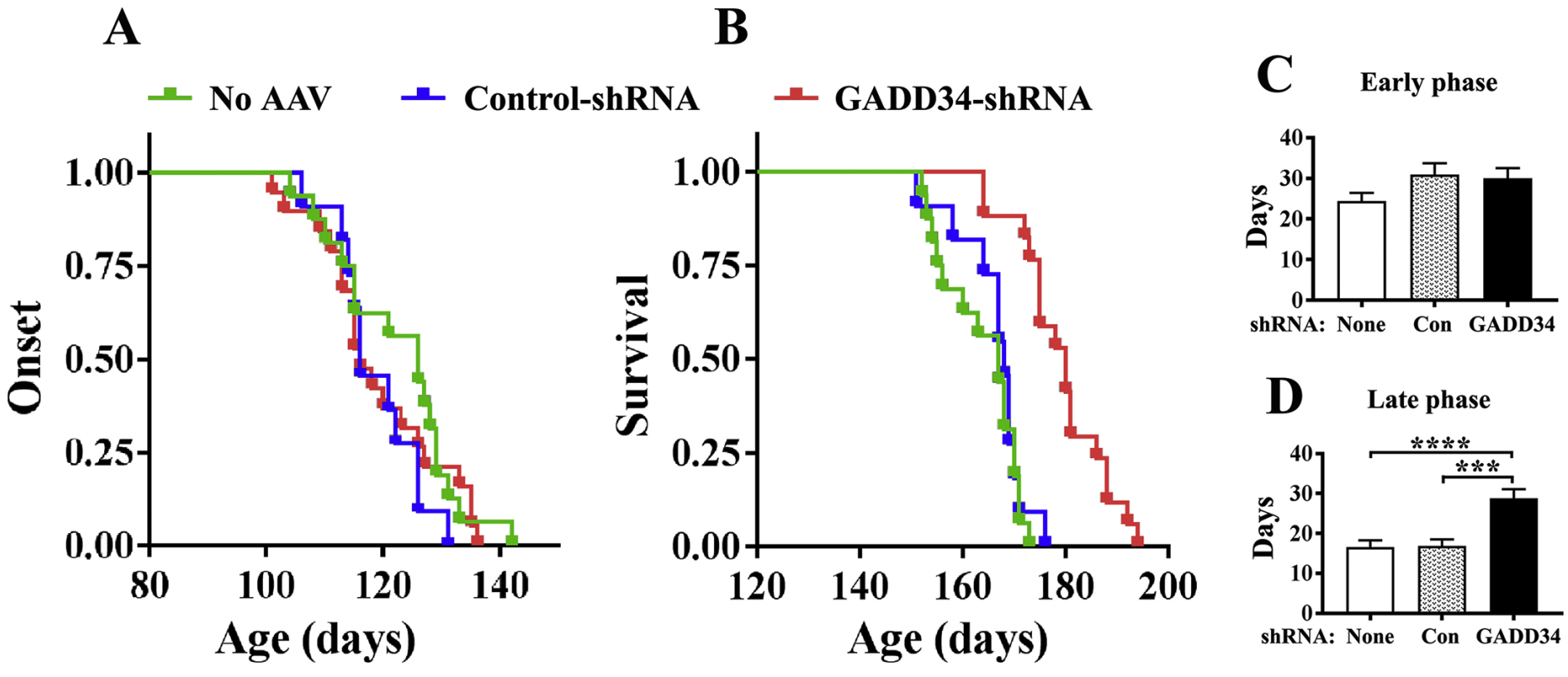
A
No AAV
Control-shRNA
GADD34-shRNA
Onset
1.00
0.75
0.50
0.25
0.00
80
100
120
140
Age (days)
B
Survival
1.00
0.75
0.50
0.25
0.00
120
140
160
180
200
Age (days)
C
Early phase
Days
40
30
20
10
0
shRNA: None
Con
GADD34
D
Late phase
****
***
Days
40
30
20
10
0
shRNA: None
Con
GADD34

Figure 4

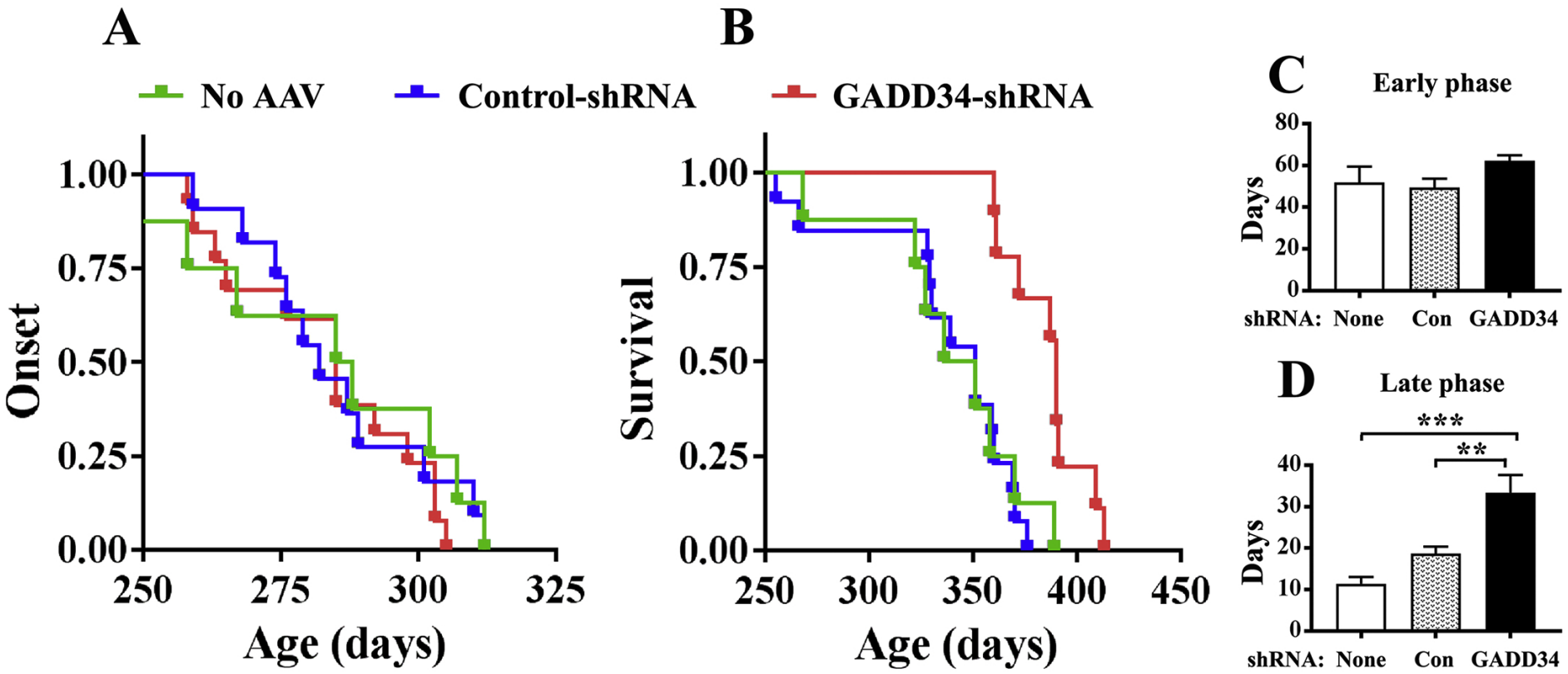
A
No AAV
Control-shRNA
GADD34-shRNA
Onset
1.00
0.75
0.50
0.25
0.00
250
275
300
325
Age (days)
B
Survival
1.00
0.75
0.50
0.25
0.00
250
300
350
400
450
Age (days)
C
Early phase
Days
80
60
40
20
0
shRNA: None
Con
GADD34
D
Late phase
***
**
Days
40
30
20
10
0
shRNA: None
Con
GADD34

Figure 5

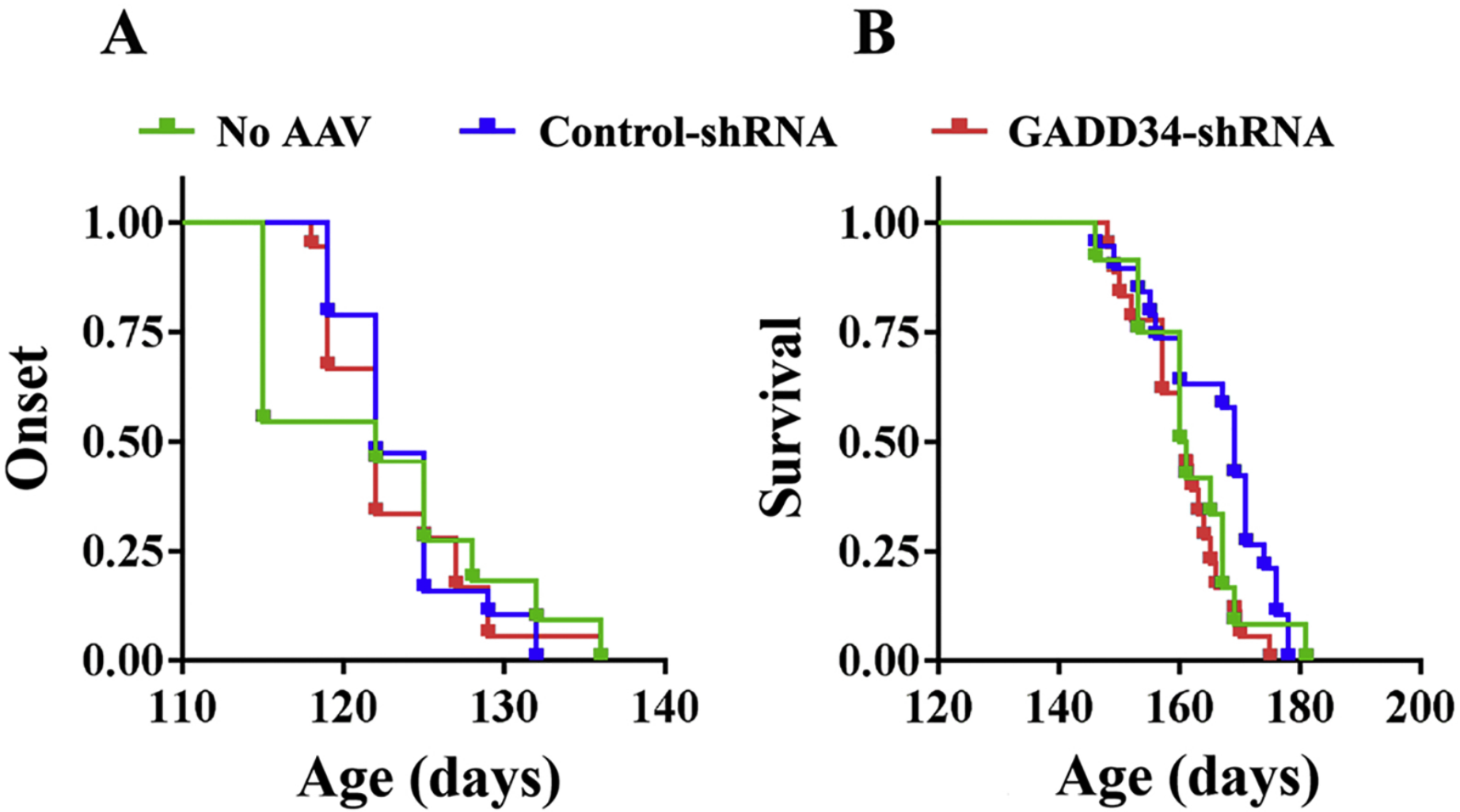
A
No AAV
Control-shRNA
GADD34-shRNA
Onset
1.00
0.75
0.50
0.25
0.00
110
120
130
140
Age (days)
B
Survival
1.00
0.75
0.50
0.25
0.00
120
140
160
180
200
Age (days)

Figure 6

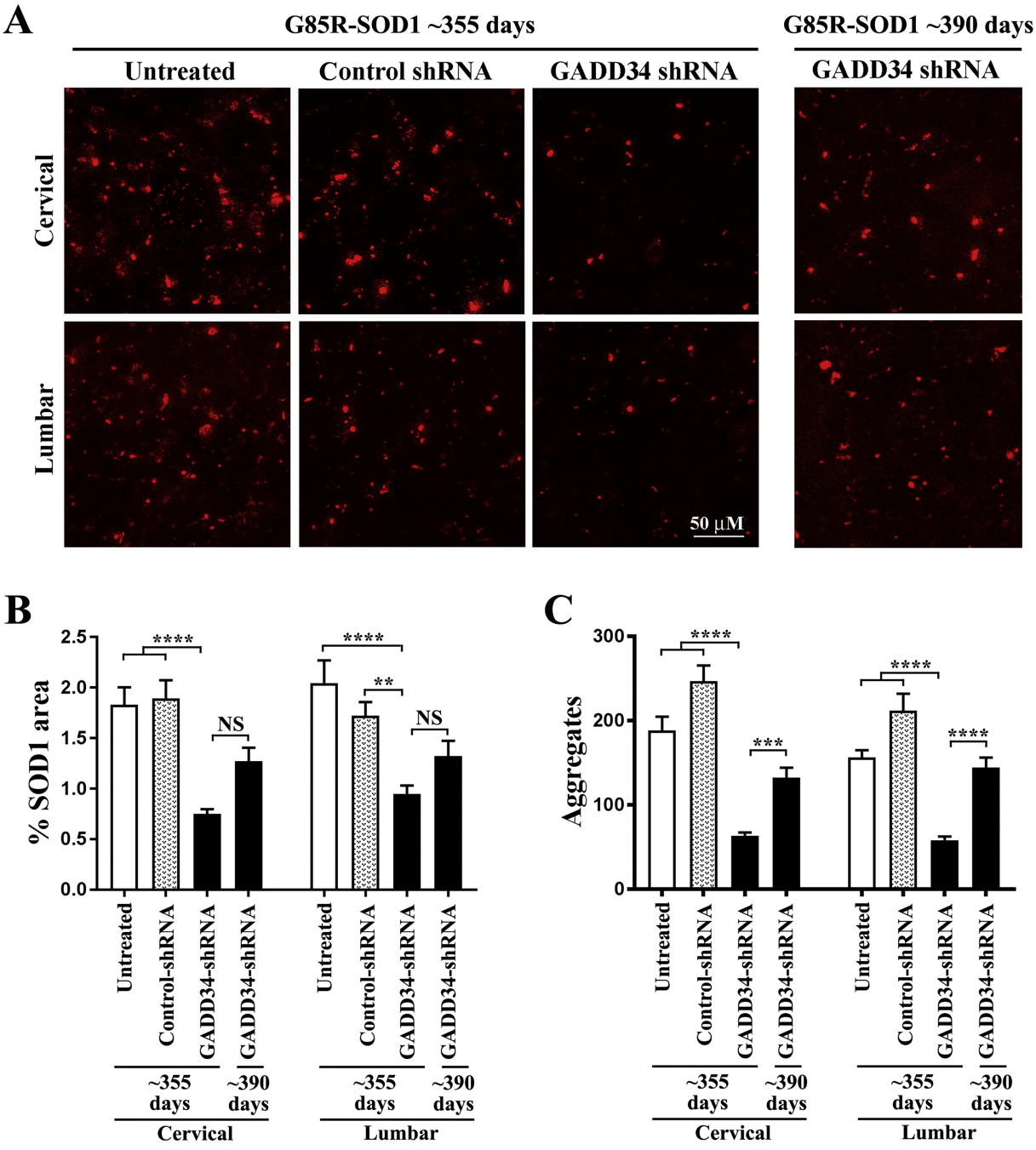
A
G85R-SOD1 ~355 days
G85R-SOD1 ~390 days
Untreated
Control shRNA
GADD34 shRNA
GADD34 shRNA
Cervical
Lumbar
50 µM
B
% SOD1 area
2.5
2.0
1.5
1.0
0.5
0.0
****
****
**
NS
NS
Untreated
Control-shRNA
GADD34-shRNA
GADD34-shRNA
Untreated
Control-shRNA
GADD34-shRNA
GADD34-shRNA
~355 days
~390 days
~355 days
~390 days
Cervical
Lumbar
C
Aggregates
300
200
100
0
****
***
****
****
Untreated
Control-shRNA
GADD34-shRNA
GADD34-shRNA
Untreated
Control-shRNA
GADD34-shRNA
GADD34-shRNA
~355 days
~390 days
~355 days
~390 days
Cervical
Lumbar

Figure 7

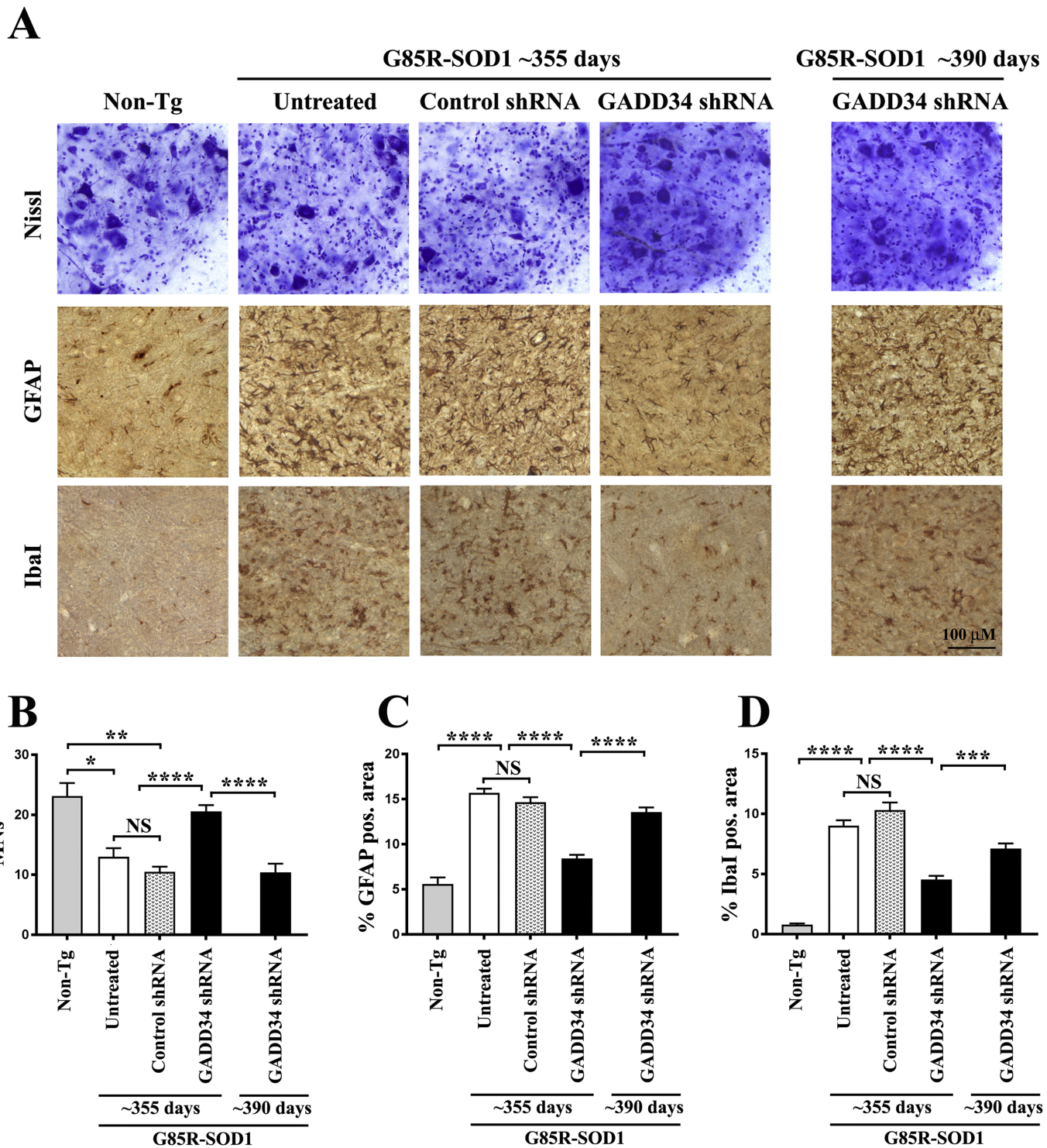
A
G85R-SOD1 ~355 days
G85R-SOD1 ~390 days
Non-Tg
Untreated
Control shRNA
GADD34 shRNA
GADD34 shRNA
Nissl
GFAP
IbaI
100 μM
B
MNs
C
% GFAP pos. area
D
% IbaI pos. area
NS
*
**
***
****
Non-Tg
Untreated
Control shRNA
GADD34 shRNA
GADD34 shRNA
~355 days
~390 days
G85R-SOD1

Figure 8